

Is there a positive feedback between Arctic stratus
and Arctic sea ice changes?
Master thesis

Mari Fenn Kristiansen

Abstract

This will be my abstract.

Write it later....

No more than a page and should contain:

- main findings - how it compares to others - a conclusion?

Acknowledgements

First of all I want to thank my main supervisor Jón Egill Kristjánsson for an interesting project and for the opportunity to come and work at NCAR for a couple of weeks. I also want to thank my other supervisor Kari Alterskjær for her "poking" and setting deadlines and pushing me for the last six months. I greatly appreciate their guidance and criticism throughout this project, and the doors that were always safe to knock on. Thank you so much to Anne Claire Fuillioux for helping me with setting up and getting started with WRF, and to both her and Kjell Andresen for help with technical problems during my work with this thesis. Thanks also to Gregory Thompson whom Jón Egill and I met with in Boulder, for meeting with us and answering all my e-mails about running the new aerosol-aware microphysics scheme in WRF. These past two years have been very enjoyable in all their stress thanks to Marta and Helle especially, for all their positiveness. Last, but not least, I would like to thank Henrik, for great technical help and moral support.

Husk å takke Kjetil også :)

Contents

1	Introduction	1
1.1	Main goal	1
1.2	My contribution	2
1.3	Area description	2
1.4	Background	3
1.5	Structure of the thesis	4
2	Theory of Clouds and Radiation	5
2.1	Arctic clouds	5
2.2	Cloud effects on radiation	6
2.2.1	The Cloud – a gray body	7
2.2.2	Cloud optical depth	7
2.2.3	Cloud droplet effective radius	8
2.2.4	Liquid Water Content and Path	8
2.3	Aerosols and clouds	9
2.3.1	The first indirect effect	10
2.3.2	The second indirect effect	10
2.3.3	Aerosol-cloud interactions	10
3	Model and methods	11
3.1	Description of the WRF-ARW Modeling System	11
3.1.1	The vertical coordinate	13
3.1.2	Staggered grid	13
3.2	Model setup	15
3.2.1	Choices of physics in the model	16
3.3	Model runs	18
3.3.1	Manipulation of input files	19
3.4	Input data	19
3.5	Processing of the results	20

4 Results and discussion	21
4.1 Reference figures from the control run	21
4.2 Consequences of removal of sea ice, without manually changing the aerosol concentration	21
4.3 What about if we left the sea ice unchanged, but increased the aerosol number concentration by a factor of 10 for the whole period?	25
4.4 Day 5, with no ice, and unchanged aerosols	26
4.5 Day 5, sea ice unchanged and aerosol concentration multiplied by 10	27
4.6 The control run figures!	28
5 Summary and Conclusions	35

Chapter 1

Introduction

Low clouds have a net warming effect in the Arctic [Intrieri *et al.*, 2002b], as opposed to the well known net cooling effect they have at lower latitudes. Low layered clouds (stratus) also dominate the Arctic cloud cover. The Arctic climate changes have been greater than the global mean and have become known by the term "Arctic amplification" [Graversen *et al.*, 2008]. Therefore the climate effect of low clouds in the Arctic is an interesting topic to study.

Decreasing sea ice extent could lead to an increase in the aerosol number concentrations in the area where ice has retreated. The open sea surface it self would lead to an increase in release of sea salt and DMS (dimethyl sulfide) to the lower atmosphere. The lack of sea ice would also increase the likelihood that the sea could be used for shipping, which would pollute the area.

The enhancement of evaporation from diminishing sea ice and the increase in aerosol number concentration from open water and shipping could lead to denser and longer-lived low clouds in the area of sea ice retreat. A followup question to that is if these clouds would then have a slightly different radiative effect, and by that influence the further retreat of sea ice.

1.1 Main goal

According to the IPCC report by Boucher *et al.* [2013] the study by Eastman & Warren [2010a] using visual cloud reports from the Arctic, with surface and satellite observations, and the studies by Kay & Gettelman [2009] and Palm *et al.* [2010] using lidar and radar observations have confirmed that the low-cloud amount over the Arctic oceans varies inversely with sea ice amount.

This means that there is an increase in cloud amount when there is less sea ice. Now what we want to know is if these clouds are also denser and more persistent, and could lead to an enhanced warming and reduced sea ice amount, a positive feedback.

With this thesis I try to find if a decrease in Arctic sea ice lead to denser and more persistent clouds. It has been suggested that the decline in sea ice extent would allow for more pollution in the Arctic, as a consequence of more open water and ship traffic. The effect of increase in aerosol concentrations from shipping and open water, and the effect of enhanced evaporation from open water are studied separately and combined. With the main goal to find if this would lead to changes in clouds that could enhance downwelling long wave radiation and decrease upwelling short wave radiation, both of which have warming effects.

1.2 My contribution

The findings in my thesis have been achieved with some of the most recently developed code (by Greg Thompson [Thompson & Eidhammer, 2014]) for cloud micro physics and aerosols and their effects on radiation, in modeling. The results build further on the work of other researchers @name-some-and-cite and may raise some questions for further research within the field.

1.3 Area description

The area of the study in this thesis is in the Arctic, north of the United States of America and north-west of Canada. The study area covers the Beaufort Sea and small parts of Alaska and Canada, and can be seen in figure 1.1.

There are a few reasons for choosing this as the study area. First it is in the Arctic, and sea ice is present there in autumn, even in 2012 when there was record low sea ice extent. Also it has been exposed to field campaigns: Surface Heat Budget of the Arctic Ocean (SHEBA) [Uttal *et al.*, 2002], First International Satellite Cloud Climatology Project Regional Experiment Arctic cloud Experiment (FIRE ACE) [Curry *et al.*, 2000], Mixed-Phase Arctic Cloud Experiment (M-PACE) [Verlinde *et al.*, 2007] and more. Therefore there are many studies on Arctic clouds that include this study area and data from some of the mentioned field campaigns. This provides parts of the science basis for my study and selection of literature and studies for comparison and questions. Quite a few studies are based on satellite data

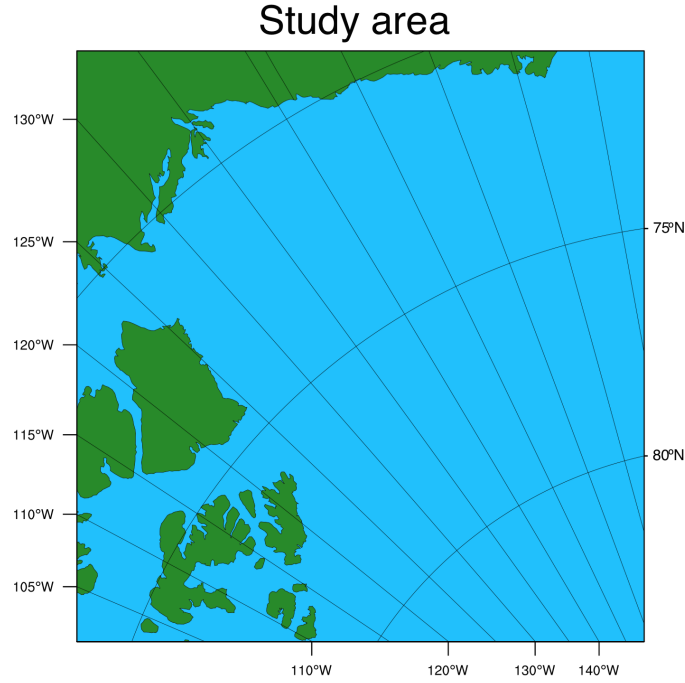


Figure 1.1: An overview of the study area. The bottom right corner is the northernmost point and the y-axes show longitude and latitude to the left and right, respectively.

analysis and some of them are presented in the next chapter as background and motivation for my thesis.

1.4 Background

In this chapter I shall present some recent literature on the subject, that forms a basis for the study presented in this thesis.

A study by Schweiger *et al.* [2008] investigated the connection between sea ice variability and cloud cover over over the Arctic seas during autumn. They analysed the ERA-40 re-analysis products and some satellite data sets. They found that that sea ice retreat was linked to a decrease in low-level (surface to ~ 1.9 km) cloud amount and an increase in mid-level (~ 1.9 to 6.1 km) clouds. They state that the decrease in static stability and deepening of the atmospheric boundary layer, following ice retreat, contribute to the rise in cloud level.

The study by Vavrus *et al.* [2010] investigated the behaviour of clouds, during intervals of rapid sea ice loss in the Arctic in the 21st century. The study was done by use of the Community Climate System Model (CCSM3). Their results support that cloud changes appear to accelerate rapid loss of sea ice in autumn, and possibly in winter. They also conclude that "the trends in total cloudiness during rapid ice loss events are explained almost entirely by low-level clouds" and that "a positive feedback from primarily low cloud changes amid a warming climate".

Kay & Gettelman [2009] combined satellite data and complementary data sets to study the Arctic cloud and atmospheric structure during summer and early Autumn over the years 2006-2008. This covers the at the time record low sea ice extent from 2007. In contrast to the study by Schweiger *et al.* [2008] they found more low-level cloud. There are reasons to believe that the observations used in their study are more accurate than the re-analysis used in Schweiger *et al.* [2008].

Eastman & Warren [2010b] analysed visual cloud reports from the Arctic for year-to-year variations and found that following a low-ice September there would be enhanced low cloud cover.

The study by Palm *et al.* [2010] using satellite and lidar data and found that areas of open water were associated with greater polar cloud fraction.

A common uncertainty and missing link in a few of these studies is that they did not look at liquid water content, effective radii and other parameters affecting the radiative properties of the clouds. In this study, that is what I want to look in to, how these properties are influenced by the changing sea ice, and if the clouds enhance the sea ice melt.

1.5 Structure of the thesis

In the following chapter, Chapter 2, the most important theory needed to understand some of the processes in clouds and their possible effect on the sea ice is presented. Chapter 3 is where I explain which model and tools and I have used and how I have worked with them to get the results presented and discussed in chapter 4. A summary of main findings and conclusions are presented in the last chapter 5, before the list of references at the very end.

Chapter 2

Theory of Clouds and Radiation

In this chapter, a brief overview of clouds in the Arctic, with focus on stratus, is presented first. Followed by how cloud properties can influence radiation. Last in this chapter, a section on aerosol-cloud interactions is included.

2.1 Arctic clouds

The Arctic cloud cover is dominated by low clouds, and the largest amounts of low stratus clouds are over the open oceans [Klein & Hartmann, 1993]. According to Klein & Hartmann [1993] stratus in the Arctic basin peaks during summer at nearly 62%, while during the winter season the stratus only accounts for 18% of the cloud cover. This leads them to conclude that the seasonal cycle of stratus in the Arctic is driven by the temperature cycle, thereby moisture content in the atmosphere, rather than the static stability.

Low clouds have bases below 2000 m. Stratus (St) are layered clouds that form when extensive areas of stable air are lifted. Stratus clouds are normally between 0.5 and 1 km thick, whereas they can be several km wide [Aguado & Burt, 2010].

The air in the Arctic is very stable in winter (polar night), and clean since there are not many sources for pollution. In Autumn the sea ice extent reaches a minimum after the summer melting and leaves open water to influence low clouds and their properties. Some of the cloud radiative properties are presented in the next section.

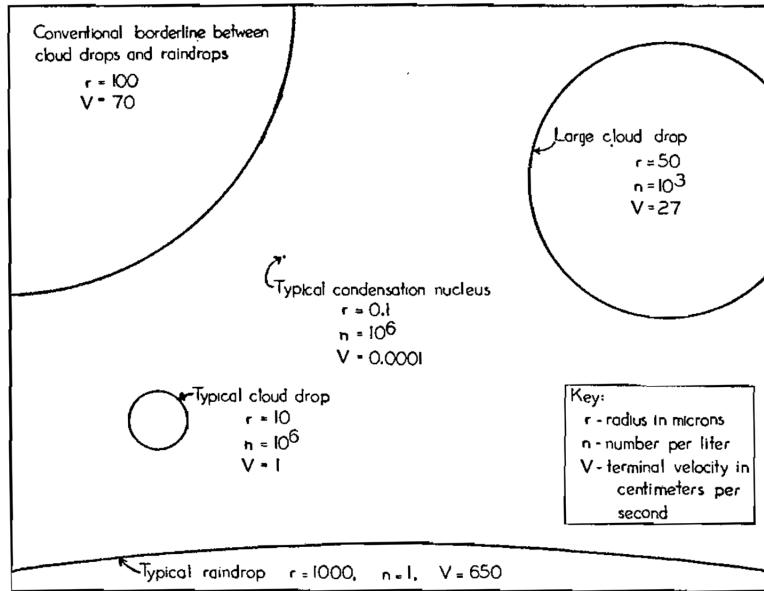


Figure 2.1: Size of CCN, typical cloud droplet, large cloud droplet, borderline between cloud droplets and raindrops and typical size of raindrop. From [McDonald, 1958].

2.2 Cloud effects on radiation

Is this where I should include the part about heating (not cooling) effect of low cloud in the Arctic, as opposed to global mean which is cooling?

As mentioned in Chapter 1 there is no solar radiation to reflect during winter and the polar night in the Arctic, whereas in the summer the zenith angle is so high that even though there is sunlight 24 hours a day the cooling effect in summer does not average out the heating effect the clouds have in winter. A high zenith angle, means that the radiation has to travel through more atmosphere, which gives a higher optical depth and stronger depletion of the radiation beam. Consequently, the low clouds' ability to absorb and emit terrestrial radiation dominates over their reflective effect on the solar radiation.

The cloud microphysical properties that determine the cloud radiative properties include: the amount of condensed water, the size and shape of the cloud particles, and the phase of the particles/and if the particles are liquid or ice [Curry *et al.*, 1996].

2.2.1 The Cloud – a gray body

Stefan–Boltzmanns law states that the flux density emitted by a blackbody is proportional to the fourth power of the absolute temperature [Liou, 2002].

$$F = \epsilon_\lambda \sigma T^4 \quad (2.1)$$

where $\epsilon_\lambda = 1$ is the emissivity for a blackbody at wavelength λ . $F[W\ m^{-2}]$ is the flux density emitted by the body, and $\sigma = 5.67 \cdot 10^{-8} Jm^{-2}sec^{-1}deg^{-4}$ is the Stefan–Boltzmann constant. A blackbody both absorbs and emits at maximum, and the ratio of absorption and emission to the maximum is given by the absorptivity, α_λ , and the emissivity, ϵ_λ , for wavelength λ . Kirchoff's law states that the absorptivity and emissivitvty for a medium are equal for each wavelength: $\alpha_\lambda = \epsilon_\lambda$. Kirchoff's law is only applicable at local thermodynamic equilibrium in the lower 60-70 km of the atmosphere. Since this study focuses on the lowest 2-3 km of the troposphere, the law is applicable.

A cloud can be defined as a a gray body, which means that α_λ and ϵ_λ are not maximum, $\alpha_\lambda = \epsilon_\lambda < 1$ [Liou, 2002].

Since the gray body does not have maximum absorption, some of the radiation flux incident on the medium must be reflected. For a cloud this is represented by the cloud albedo, given by

$$A = \frac{(1-g)\tau}{1 + (1-g)\tau} = \frac{1-g}{\frac{1}{\tau} + (1-g)} \quad (2.2)$$

So now I have to explain about the asymmetry factor (g) and the single scattering albedo ($\tilde{\omega}$) which has been approximated to one for this equation to be valid for the cloud albedo. According to Twomey, $g=0.8$ or 0.9 for warm clouds. $g=1$ is pure forward scattering and $g=-1$ is pure back-scattering. The asymmetry factor gives the direction of the scattered radiation. $g = \cos \theta$ where θ is the scattering angle. A power-averaged value of the cosine of the scattering angle [Twomey, 1974].

2.2.2 Cloud optical depth

Cloud optical depth or cloud optical thickness, τ , is a measure of the cumulative depletion that a beam of radiation directed straight downward (zenith angle $\theta = 0$) would experience in passing through a defined cloud layer. The

cloud optical depth is given by [Twomey, 1977]

$$\tau = \int_0^h k_E dz = \pi \int_0^h \int_0^\infty r^2 Q_E(r/\lambda) n(r, z) dr dz \quad (2.3)$$

at height z above cloud base for a cloud of depth h , containing $n(r)dr$ drops with radius in the interval $(r, r + dr)$ per cubic centimeter. $Q_E(r/\lambda)$ is the extinction efficiency and k_E is the extinction coefficient [Twomey, 1977]. In the visible, for $\lambda \ll r$, $Q_E \approx 2$ is a good approximation [Liou, 2002], and we get the simpler expression

$$\tau = 2\pi N r_e^2 h \quad (2.4)$$

where it is assumed that the cloud droplet radius can be approximated by the effective radius, r_e .

2.2.3 Cloud droplet effective radius

The cloud droplet effective radius determines important radiative properties of a cloud, cloud albedo (A) and cloud emissivity (ϵ) [Hansen & Travis, 1974], and is therefore of particular interest.

The cloud droplet effective radius is a weighted mean of the size distribution of cloud droplets. The effective radius may be written

$$r_e = \frac{\int r^3 n(r) dr}{\int r^2 n(r) dr} \quad (2.5)$$

where r_e is the effective radius.

2.2.4 Liquid Water Content and Path

The amount of condensed water can be expressed by the liquid water content (LWC) in the cloud, often presented with units g m^{-3} and is proportional to the cloud droplet number concentration. From Rogers & Yau [1989] we can express the number of droplets with radius r by

$$N = \int n(r) dr \quad (2.6)$$

where N is the cloud droplet number concentration (cm^{-3}), and $n(r)$ is the number of droplets with radius r . When we use the median volume radius,

\bar{r} (μm), the LWC can be written

$$LWC = \int \rho_L \frac{4}{3} \pi r^3 n(r) dr \quad (2.7)$$

$$= \frac{4}{3} \pi \rho_L \int r^3 n(r) dr \quad (2.8)$$

$$= \frac{4}{3} \pi \rho_L \bar{r}^3 \int n(r) dr \quad (2.9)$$

$$= \frac{4}{3} \pi \rho_L \bar{r}^3 N \quad (2.10)$$

where the last equation shows the proportionality of LWC to the cloud droplet number concentration N , and to \bar{r} . ρ_L is the density of liquid water.

Another common measure of condensed water is the liquid water path (LWP). If the LWC is integrated over a column, from the base to the top, it gives the LWP of that column.

$$LWP = \int_{base}^{top} LWC dz \quad (2.11)$$

The LWP is the column of liquid water in a cloud and is usually expressed by $g m^{-2}$.

A higher LWC or LWP increases the reflectivity of the cloud, and thereby reduces the SW radiation reaching the surface.

2.3 Aerosols and clouds

For low clouds to form there must be available aerosols. Aerosols act as cloud condensation nuclei (CCN) by letting water vapor condense on them. This is how a cloud droplet is formed. For an ice particle to be present in a low cloud, an ice nuclei (IN) and low temperatures are necessary. If an IN hits a cloud droplet with temperature below zero, a super-cooled droplet, the droplet will freeze.

Aerosols have a direct effect on the climate by scattering and absorbing SW radiation, and scattering, absorbing and emitting LW radiation. They also have an effect on climate through clouds, an indirect effect. The amount of CCNs and INs available affect the properties of the clouds in the area. There are two known indirect effects that aerosols have on radiation, through clouds. The first indirect effect was proposed by Twomey [1974] and is often referred to as the Twomey effect. The second indirect effect was proposed

by Albrecht [1989] and is also known as the lifetime effect.

2.3.1 The first indirect effect

If there are few CCNs in an area, a cloud formed there would be a clean cloud with few, but large droplets and therefore have a low albedo and precipitate easily. If the area had high aerosol concentration, the cloud would be polluted and have more numerous but smaller droplet, which means it would have a higher albedo and precipitation would be suppressed. The first indirect effect, suggested by Twomey [1974], describes the enhancement of cloud albedo as a consequence of an increase in aerosol content and thereby available CCNs. By increasing droplet concentration and hence the optical thickness of a cloud, see equation 3.3, pollution acts to increase the reflectance of clouds. It is clear from equation 3.3 that if the droplet concentration is increased, so is the optical thickness of the cloud.

The cloud optical depth will change with changes in aerosol number concentrations and changes in clouds and their properties. For instance if a cloud has many small droplets, the cloud optical depth will be higher. Whereas fewer cloud droplets will yield a lower optical depth, resulting in more SW radiation reaching the ground — having a warming effect on the area.

(Include a figure showing the indirect effect)

2.3.2 The second indirect effect

The second indirect effect, or the cloud lifetime effect, suggests more numerous but smaller droplets reduce the precipitation efficiency and by that enhances the cloud lifetime and hence the cloud reflectivity [Albrecht, 1989]. This effect has been estimated to be roughly as large as the first indirect effect [Lohmann & Feichter, 2005].

2.3.3 Aerosol-cloud interactions

Cloud presence is due to water vapor condensing on CCNs and possibly freezing if the aerosol's structure resembles that of an ice crystal, IN. Processes known to affect the local aerosol concentration are: precipitation because the precipitation will wash out aerosols from the air when falling through it, this is also known as scavenging. Pollution, increases in aerosol concentration might inhibit precipitation and cause longer-lived, more persistent clouds, which will in turn affect the radiation balance.

Chapter 3

Model and methods

To produce results for the thesis, a formulation of the Weather Research and Forecasting (WRF) Model called the Advanced Research WRF (ARW) has been used. The model is described in the first part of this chapter. Then follows a description of the model setup and the different physics schemes that were chosen for this study, before a summary of the different runs that were performed. Ending the chapter are two short sections on the input data and processing of the model output.

3.1 Description of the WRF-ARW Modeling System

The version of the WRF-ARW modeling system used is 3.6.1, which was released in April 2014. The model is primarily developed at the National Centre for Atmospheric Research (NCAR) in Boulder, Colorado. The ARW model is the first fully compressible conservative form nonhydrostatic model designed for both research and operational numerical weather prediction (NWP) applications [Skamarock & Klemp, 2008].

As can be seen from figure 3.1 the WRF-ARW Modeling System consists of four major programs [Wang *et al.*, 2015]:

- The WRF Preprocessing System (WPS)
- WRF-Data Assimilation (WRF-DA)
- ARW solver
- Post-processing & Visualization tools

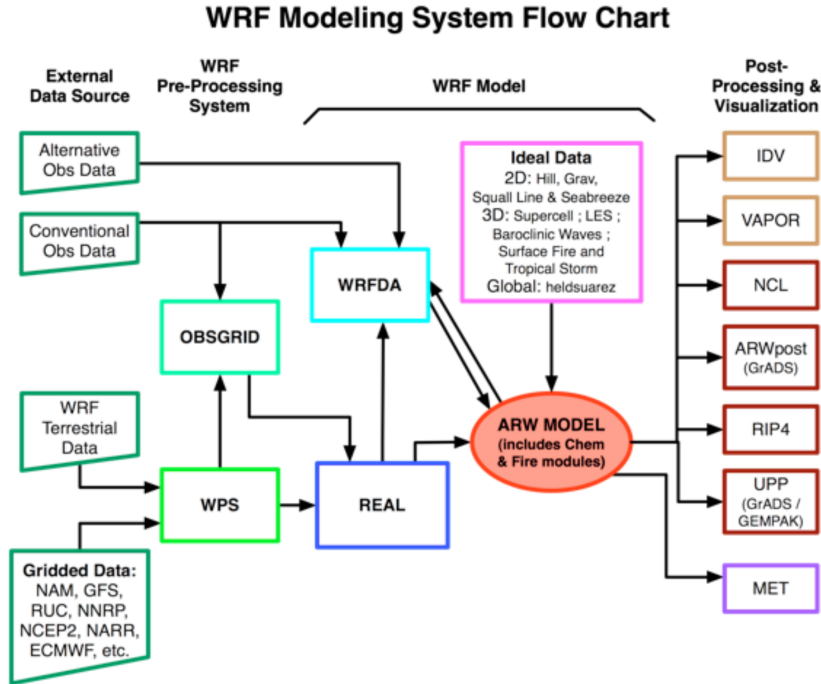


Figure 3.1: Flowchart for the WRF ARW Modeling System Version 3. From Wang *et al.* [2015].

WPS is used primarily for real data simulations [Wang *et al.* , 2015], like the study presented in this thesis. A real-data simulation means that it has been initialized by observations and reanalysis, not artificial data. WPS' functions include defining simulation domains, interpolating terrestrial data and degridding and interpolating meteorological data from another model to this simulation domain [Wang *et al.* , 2015]. WRF-DA is optional and can be used to ingest observations into the interpolated analyses created by WPS [Wang *et al.* , 2015], but was not used in this study. The ARW solver is the key component of the modeling system, which is composed of several initialization programs for idealized, and real-data simulations, and the numerical integration program [Wang *et al.* , 2015].

3.1.1 The vertical coordinate

The continuous equations solved in the ARW model are the Euler equations cast in a flux form where the vertical coordinate, η , is defined by a normalized hydrostatic pressure,

$$\eta = (p_h - p_{ht})/\mu \quad (3.1)$$

where $\mu = (p_{hs} - p_{ht})$ [Skamarock & Klemp, 2008]. p_h is the hydrostatic component of the pressure and p_{hs} and p_{ht} are the values of the hydrostatic pressure in a dry atmosphere at the surface and top boundaries respectively [Skamarock & Klemp, 2008].

The vertical coordinate is the traditional σ coordinate used in many hydrostatic atmospheric models, shown in figure 3.2.

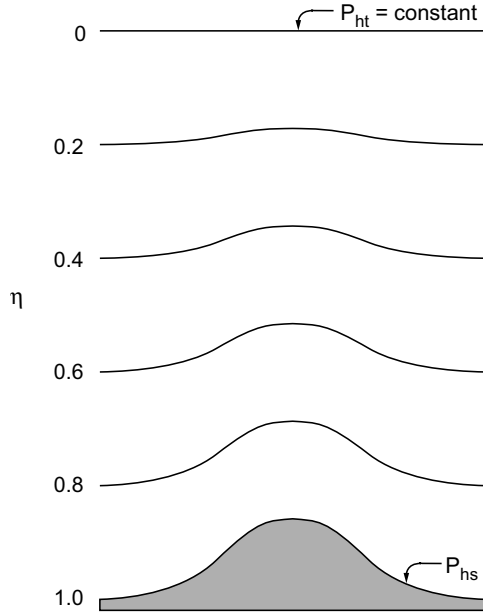


Figure 3.2: This figure is shown as presented in Skamarock & Klemp [2008], and is a schematic of the terrain following a σ coordinate. P_{hs} and P_{ht} are the hydrostatic pressure at the surface and top respectively.

3.1.2 Staggered grid

The WRF-model uses a staggered grid, which means that some variables lie in the middle of a grid box, and others on the sides of the box. The pressure

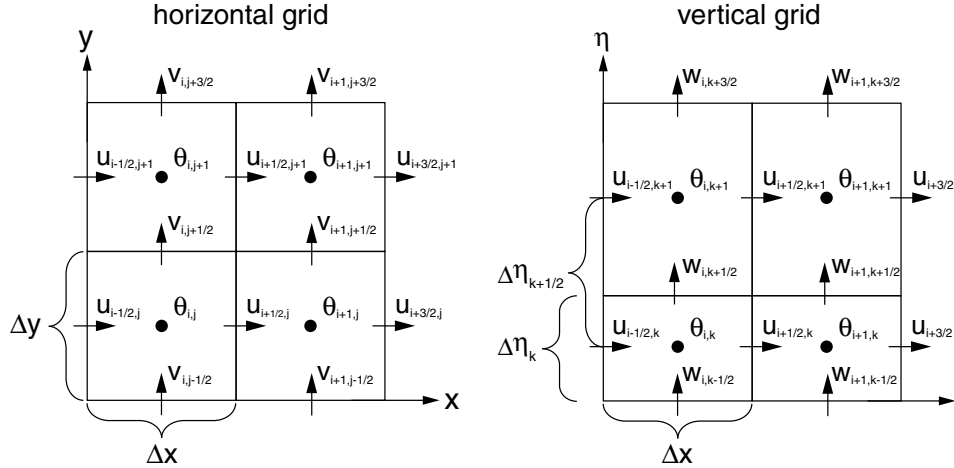


Figure 3.3: This figure is shown as presented in Skamarock & Klemp [2008], and shows the staggering for the C-grid. The horizontal staggering to the left, and the vertical staggering to the right.

for example is in the middle of the grid box, and the winds on each side of the box use the pressure in the middle of one box, and the middle of the box next to it as reference for calculating the winds at the grid box sides. A staggered grid saves computational time since the a variable at point a needs only the values at $a+1/2$, and $a-1/2$, in stead of $a+1$ and $a-1$, which is more computationally costly.

The staggered grid therefore reduces the computation time of the WRF-ARW modeling system.

This is important to know, also for the variables in the vertical. If a cloud effective radius, r_e , for example lies between two levels, in the middle of a layer, or if they have values exactly on the levels.

Figure 3.3 shows the staggered C-grid used in the WRF-model. The C-grid is the most used staggered grid in nonhydrostatic NWP and research models [Skamarock & Klemp, 2008].

The selection of physics schemes in WRF-ARW are numerous. The choice of schemes treating microphysics in clouds and aerosols, and the radiation are presented in the following section about the model setup.

3.2 Model setup

The model was ran with a $4 \text{ km} \times 4 \text{ km}$ horizontal grid point spacing, with 300×300 grid points, and 72 vertical layers, with the model top at 10 hPa. The area covers parts of the Beaufort Sea, by Canada and Alaska. This area was chosen because data from the area has been used for related studies [Intrieri *et al.*, 2002a, Kay & Gettelman, 2009, Palm *et al.*, 2010, Schweiger *et al.*, 2008, Shupe & Intrieri, 2004, Wu & Lee, 2012] as mentioned in Chapter 1 and described in Chapter ???. The area is not completely ice free any part of the year, and provides a good place to simulate cloud-sea ice interaction. The area is over several time zones but is approximately 7 hours behind UTC time. The times given in the WRF-ARW modeling system are UTC. The model was ran for a period of 5 days, 1st to 6th of September 2012. This is approximately when the record low ice extent in the Arctic was set (eg. National Snow and Ice Data Centre, U.S.A., Beitler [2012]).

The vertical layers in the ARW model are often referred to as eta levels, because of the choice of η as the vertical coordinate. These levels have uneven vertical spacing. The fact that this η is the traditional σ -coordinate, means that the altitude of each level is dependent on pressure, therefore the level height varies in both time and space. As a consequence of pressure dependence, the levels in the lower troposphere are closer to each other than the levels higher up in the troposphere. Therefore the low clouds in the area can be resolved. Approximate heights for the lowest 11 eta levels is shown in Table 3.1.

Table 3.1: Approximate height for each level in meters above the surface.

Eta level	Approximate height
1	10 m
2	50 m
3	130 m
4	230 m
5	370 m
6	530 m
7	650 m
8	950 m
9	1250 m
10	1400 m
11	1600 m

3.2.1 Choices of physics in the model

The physics options in WRF fall into several categories, each containing several choices. Table 3.2 shows some of the different categories and the choice of scheme, for this study, within each of those categories.

Table 3.2: Table of physics categories and choice of scheme for this thesis

Physics categories	Scheme selected within category
(1) microphysics	aerorol-aware [Reisner <i>et al.</i> , 1998, Thompson & Eidhammar, 2014, Thompson <i>et al.</i> , 2004, 2008]. Option 28.
(2) cumulus parameterization	Grell 3D @cite authors. Option 5.
(3) planetary boundary layer (PBL)	Yonsei University scheme @cite authors. Option 1.
(4) land-surface model	Noah Land Surface Model @cite authors. Option 2.
(5) radiation	RRTMG LW & SW [Iacono, 2003, Iacono <i>et al.</i> , 2000, 2008, Mlawer <i>et al.</i> , 1997]. Radiation options 4.

The ARW model offers a wide selection of schemes to treat different physics that one wants represented in the model. The schemes treat the physics slightly differently and some schemes are better for certain horizontal and vertical resolutions than others, so one needs to be careful when choosing how the model is to treat the physics. For my thesis, the especially relevant scheme to mention is the cloud microphysics scheme that I chose, which is the aerosol-aware scheme described in Thompson & Eidhammar [2014]. When studying cloud and rediation response to removal of sea ice we might expect an increase in aerosols from the open ocean and increased sea traffic. The aerosols are therefore also relevant for the choice of schemes, and the aerosol-aware scheme includes the necessary processes for this study.

The aerosol-aware scheme

The microphysics includes explicitly resolved water vapor, cloud, and precipitation processes. The aerosol-aware scheme was chosen so that the study would have scavenging of aerosols included and have proper enough representation of aerosols to study aerosol-cloud interactions, without using the WRF model coupled with chemistry (WRF-Chem). According to the ARW

User's Guide by Wang *et al.* [2015], the aerosol-aware scheme considers water- and ice-friendly aerosols, and a climatological dataset may be used to specify initial and boundary conditions for the aerosol variables. I have used this climatological dataset, which is explained in Section 3.4 Input data. The scheme uses a monthly mean for aerosol number concentrations derived from multi-year (2001-2007) global model simulations in which particles and their precursors are emitted by natural and anthropogenic sources and are explicitly modeled with multiple size bins for multiple species of aerosols by the Goddard Chemistry Aerosol Radiation and Transport (GOCART) model [Thompson & Eidhammer, 2014]. The aerosol-aware scheme [Thompson & Eidhammer, 2014] is built on the schematic shown in figure 3.4, from Reisner *et al.* [1998]. It is a double moment scheme, which means it computes both mass mixing ratios, Q , and number concentrations, N , for the same water species (hydrometeors).

Figure 3.4 show the processes in the microphysics scheme developed by Reisner *et al.* [1998], which the first bulk microphysics scheme by Thompson [Thompson *et al.* , 2004] was based on. The aerosol-aware scheme [Thompson & Eidhammer, 2014] is an extension of the updated Thompson bulk microphysics scheme described in Thompson *et al.* [2008]. The figure shows a schematic of five hydrometeors, cloud water (c), rain (r), ice (i), snow (s) and graupel (g), and if just the mass mixing ratio is calculated or if both the mass mixing ratio and the number concentration is calculated. For each of the hydrometeors, prognostic equations are used with all the sources and sink terms included.

The RRTMG radiation schemes

According to Thompson & Eidhammer [2014] the Rapid Radiative Transfer Model (RRTM) for General Circulation Models (GCMs) (RRTMG) schemes for SW and LW [Iacono, 2003, Iacono *et al.* , 2000, 2008, Mlawer *et al.* , 1997] are the only radiation schemes which include the effects of the effective radii calculated in aerosol-aware. These were therefore used in combination with the aerosol-aware cloud microphysics scheme. The RRTMG schemes are accurate schemes using look-up tables for efficiency, and accounts for multiple bands and microphysics species, and includes the Monte Carlo Independent Column Approximation (MCICA) method of random cloud overlap [Wang *et al.* , 2015].

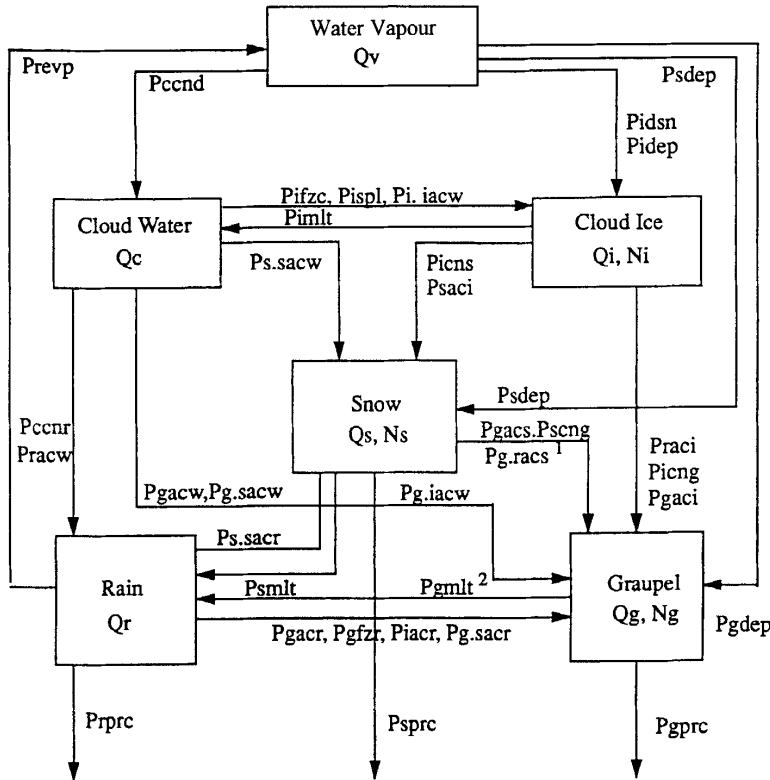


Figure 3.4: Cloud microphysical parameterization scheme typically used in NWP models as shown in Reisner *et al.* [1998]. A full list of the acronyms used in the schematic can be found in Reisner *et al.* [1998].

3.3 Model runs

The results presented in the next chapter are based on six different runs. The control run is the run where the aerosol climatological dataset has been used unchanged, and where the sea ice is kept as it was in the downloaded input data, see Section 3.4. The control run is used as a base to compare the other runs to, those with no ice and/or increased aerosol number concentrations.

There are three runs where the sea ice was removed, NoIce, Aero10NoIce and Aero100NoIce. The point of this is to compare the run with no ice to the control run, and see if there are any changes in the cloud properties, and SW and LW fluxes. For two of those runs the aerosol number concentration was also increased, these can be compared with the control run, and the other

runs that have ice, but the same aerosol number concentrations.

The number of water- and ice-friendly aerosols were multiplied by 10 and 100 both with and without sea ice for 4 runs in total: Aero10 and Aero100 with ice, and as mentioned above, Aero10NoIce and Aero100NoIce without ice. The goal is to find changes in cloud properties, and radiation fluxes compared to those in the control run.

Table 3.3 shows an overview of the different runs that have been executed, whose output have been used for production of figures presented in the next chapter.

Table 3.3: Table showing the names of the runs and if they have sea ice or not, and if the aerosol concentration has been increased by a factor of 10 or 100 through input files. All the runs have the same horizontal resolution of 4 km×4 km, dimensions 300×300, 72 vertical layers and time step 24 s.

Name	Sea ice	Aerosol concentration
control	initial	climatology
NoIce	removed	climatology
Aero10	initial	climatology×10
Aero10NoIce	removed	climatology×10
Aero100	initial	climatology×100
Aero100NoIce	removed	climatology×100

3.3.1 Manipulation of input files

The input files for the ARW solver, created by WPS and REAL (see figure 3.1) were manipulated by use of the NetCDF Operator (NCO) tool ncap2. In these files the sea ice was removed for the runs without sea ice (NoIce, Aero10NoIce, Aero100NoIce) and the aerosol number concentration from the climatological dataset was multiplied by 10 and 100 for the runs with increased aerosol concentrations by a factor of 10 and 100 respectively.

3.4 Input data

The model runs were initialized with data downloaded from the European Centre for Medium-Range Weather Forecasts (ECMWF). The downloaded data is from the ERA-Interim dataset, which is a global atmospheric reanalysis from 1979 to present and continues to be updated in real time. Through

WPS the data from ERA-Interim was interpolated over the area, with a 2 degree minute spacing between the points, to be used to initialize the model. The data used is in 6-hourly atmospheric fields on pressure levels, for the first five days of September 2012, which was the period the model was run for. This is done to make sure the initial meteorological conditions are the same in every run, so that the effects of changing a variable in the input files for the modeling system are only due to that change.

To use the climatological aerosol dataset, the file containing monthly means had to be called through WPS. The aerosol input data includes mass mixing ratios of sulfates, sea salts, organic carbon, dust, and black carbon from a 7-yr simulation with 0.5° longitude by 1.25° latitude spacing [Thompson & Eidhammer, 2014].

3.5 Processing of the results

Figures presented in my thesis, I made (unless other is stated) by use of NCL (National Centre for Atmospheric Research (NCAR) Command Language) and/or MatLab. For the NCL scripts I found a lot of help and inspiration from the example scripts for WRF-users available at ([URL for examples](#)).

Chapter 4

Results and discussion

In this chapter I will present the findings made in this study. The daily averaged differences have been calculated by subtracting the field from the control run for one time from the same field at the same time from a different run, these differences have then been added together and divided by the number of differences that were added together.(@insert equation for clarity?)

4.1 Reference figures from the control run

First we want to have something to compare with and to look back to when studying the differences from the control run to the runs with changed sea ice and/or aerosol concentration. I shall include figures for diurnally averaged fields of LWP, r_e of cloud droplet, cloud droplet number concentration (CDNC), both LW and SW up at the TOA and down at the surface. Also the IWP, cloud ice number concentration (CINC), and r_e of snow and ice may be of interest. In addition, the state of the weather situation should be considered when interpreting the results. Therefore maps with wind barbs for the wind at 10 m height and temperature at 2 m are included in this section. (De ligger i slutten av kapittelet foreløpig, slik at de ikke er i veien for leseren utover i teksten.)

4.2 Consequences of removal of sea ice, without manually changing the aerosol concentration

Lets start with average difference in LWP for NoIce - Control, day 2 (day 1 has been left out of this discussion to avoid the spin-up time. (I want to look

more closely into day 1 as well, which is when the atmosphere is still almost the same as it was for the control run, will be included in next draft.) There is a slight difference in LWP for the whole field (2.04gm^{-2} , see figure 4.3), but the area of interest in this case is where the sea ice is no longer present. There the increase in LWP is significantly higher, $>25\text{gm}^{-2}$ for the most northern part (which is in the bottom right corner). This implies that there is a new cloud forming in that area, that could not form when there was sea ice. The removal of the sea ice has allowed for increased evaporation and an increase in latent heat (LH) flux which can be seen from figure 4.2, where the area that sea ice was removed from is obvious. The northernmost part of the study area also has an increase in the cloud droplet number concentration (CDNC), figure ??, with about the same shape and size as the LWP, which fits well with equation 4.1, which we know from the theory presented in chapter 2.

$$LWC = \frac{4}{3}\pi\rho r_e^3 N \quad (4.1)$$

The amount of liquid water is proportional to the number concentration, and the LWP is the integral over the LWC, where we recall that N is the CDNC. The average increase in the CDNC would be approximately 5 droplets per cubic centimeter. The figure shows the numbers with units $10^6/\text{kg}$, which can be approximated to the more common units for CDNC, per cubic centimeter (cm^{-3}). If we assume that we are close enough to the surface to assume a pressure $p = 1000\text{hPa}$, and thereby the density to be $\rho_a = 1\text{kg}/\text{m}^3 = 1\text{kg}/10^6\text{cm}^3$, then we could write $CDNC : 10^6/\text{kg} = \text{cm}^{-3}$. Since this is the average over 11 layers, to a height of about 1600 m, the cloud could be in just a few of those layers, and have a CDNC of approximately 25 cm^{-3} if it stretches over two layers for example. The increase in effective radius in the same area also indicates the formation of a new cloud, figure 4.1, that could not form in the control run (see figure ??), whereas now that it has formed, the droplets actually have a radius. The small "blob" at 140°W and about 81°N has decreased r_e , most likely because the cloud already was saturated in that area, which can be seen from the LWP from the control run, in figure 4.12. The possible increase in aerosols from the ocean that would then lead to an increase in CCNs would make the water in that cloud spread over more CCNs, and by that leave the droplets with a smaller r_e .

The kind of U-shape that we can see in the figure for difference in r_e is also clear in the difference in downward radiation at the ground surface, for both SW and LW. The SW radiation flux at ground surface has been reduced, which is due to the increase in LWP. This can be explained by

4.2. CONSEQUENCES OF REMOVAL OF SEA ICE, WITHOUT MANUALLY CHANGING THE AEROSOL

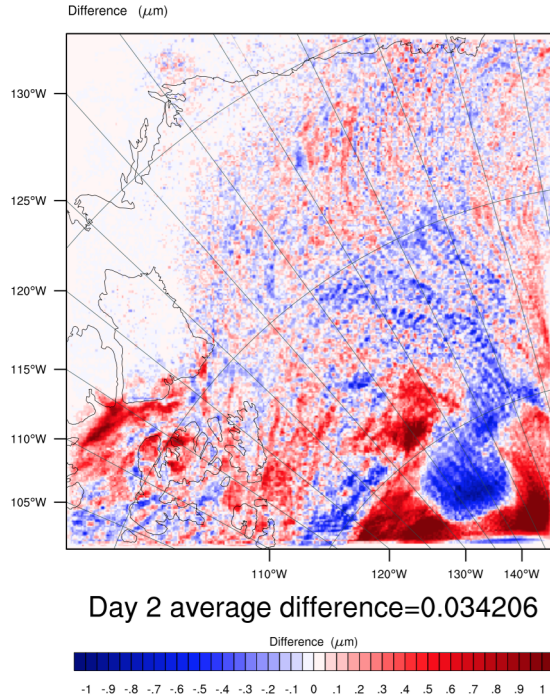


Figure 4.1: The averaged difference in effective radius of cloud droplets for the run with no ice, over the lowermost 11 layers for day 2.

equations 4.3 and 4.2, where it is clear from equation 4.2 that the cloud optical depth, τ , increases with LWP, and from equation 4.3 it is clear that an increase in τ would also increase the cloud albedo.

$$\tau = \frac{3LWP}{2\rho_l r_e} \quad (4.2)$$

$$A = \frac{1-g}{\frac{1}{\tau} + (1-g)} \quad (4.3)$$

The downward LW radiation flux at the surface has been increased due to the increase in LWP, which means that there is more water in the clouds and they emit more LW to the ground. The LW at the top of the atmosphere (TOA) does not experience such an increase, in fact it experiences a slight decrease. That it doesn't experience the same increase is explained by the Stefan-Boltzmann's law presented in chapter 2, where the flux density emitted by a body, in this case a cloud, is dependent on the temperature.

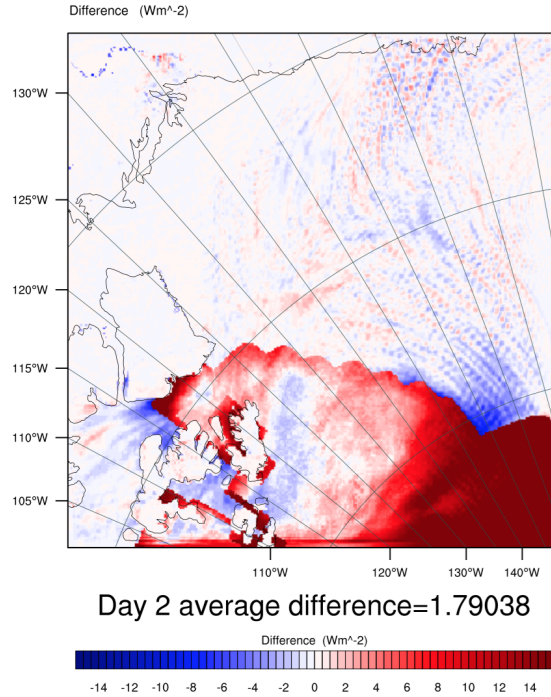


Figure 4.2: The average difference in LH flux up from the surface at day 2 .

We see from the vertical cross section showing temperature contours (@refer and make), that the temperature is higher at the surface than in the clouds, therefore the clouds have a lower emittance of LW.

Of course, the removal of sea ice would reduce the reflected SW radiation flux at the TOA, see figure 4.4. The albedo of sea ice varies between 0.5 and 0.9 depending on snow cover and the age of the ice and is typically 0.5-0.7 for bare ice, whereas a typical ocean albedo is 0.06. Thus the change in SW at TOA is mainly negative over the area of ocean where there was sea ice in the control run. The two blobs of increased SW at TOA can be recognized as the tips of the pillars in the U-shape I referred to earlier in figure 4.1 which also represent an increase in LWP and reduction in SW at surface and increase of LW at surface, this is therefore most likely due to the enhanced albedo caused by new clouds at those locations, since these figures don't show in-cloud changes, simply the difference between two fields.

The heat fluxes are almost unchanged for most of the study area by the removal of sea ice, except for the area where the sea ice has been removed (see figures 4.2 and 4.5). Especially for the northernmost part of the study

4.3. WHAT ABOUT IF WE LEFT THE SEA ICE UNCHANGED, BUT INCREASED THE AEROSOL NU

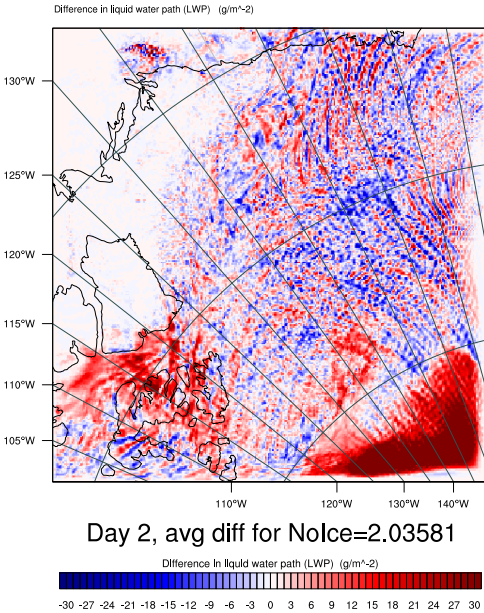


Figure 4.3: The average difference in LWP fields for day 2.

area and "sea ice removed area" the fluxes are a lot higher than in the control run. This is not surprising, since one would expect the ocean surface to hold a higher temperature than the sea ice. Also a lot more heat would be released due to evaporation than in the case when sea ice is present.

4.3 What about if we left the sea ice unchanged, but increased the aerosol number concentration by a factor of 10 for the whole period?

The increase in available CCNs leads to obvious increases in CDNC and LWP, and the expected reduction in r_e . If we look back to equation(@the one that combines LWP, effective radius and cloud optical depth). As for the NoIce run, the increase in LWP, in this case a lot higher, leads to an increase in clouds and their reflectance (albedo), therefore the SW at TOA is higher, here the signal is not disrupted by any changes made to the sea ice,

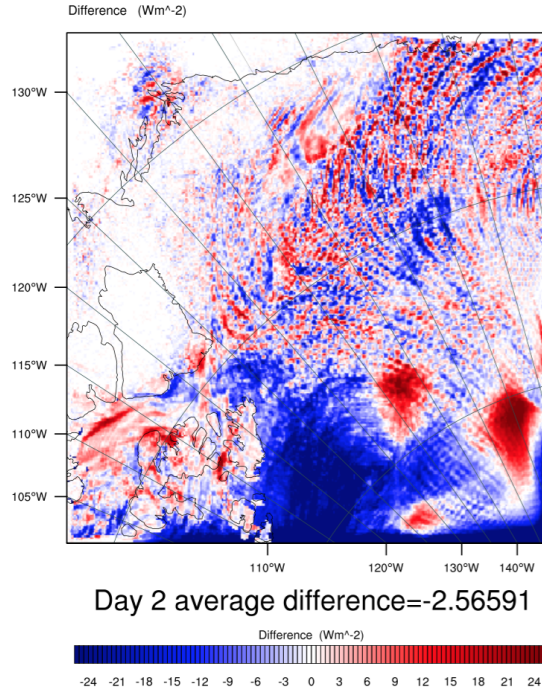


Figure 4.4: The average difference in SW flux up at TOA at day 2 .

so the increase is obvious. Thus the SW at the surface is significantly lower than in the control run. This represents a cooling of (@calculate the flux changes into temperature changes?). The average LW radiation flux at the surface is higher due to the increase in LWP and emittance by the thicker and denser(is this true) clouds.

The effect on the heat fluxes by increasing the aerosol number concentration is not clear, and probably insignificant.

4.4 Day 5, with no ice, and unchanged aerosols

Why the crap does the effective radius, LWP and CDNC go down significantly and simultaneously for the removal of sea ice at day 5?? What is up with this system? Could it be rain? From the figure I made it doesn't look like it is due to rain, 'cause it actually looks like rain is also reduced in this case, which is STRANGE!... what??? And the heat flux differences also look crazy, very clear increase right next to an equally clear decrease, the switch

4.5. DAY 5, SEA ICE UNCHANGED AND AEROSOL CONCENTRATION MULTIPLIED BY 1027

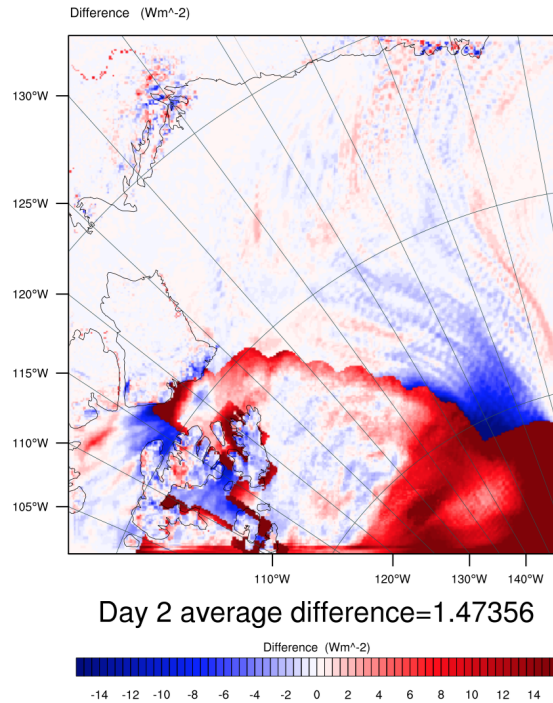


Figure 4.5: The average difference in SH flux up from the surface at day 2 .

happens at the sea ice edge. That makes sense :) but the rest doesn't!! Jon Egill suggested that I check ice and snow too, see if that can explain the difference!

4.5 Day 5, sea ice unchanged and aerosol concentration multiplied by 10

Also, why can we see the sea ice edge in the areo10-control?? The sea ice has not been changed for this run! I suggest that this is due to the decrease in SW reaching the surface, and therefore the small part of the downwelling SW radiation that is absorbed when it reaches the sea ice is smaller than when the SW is higher. Therefore the SH and LH is lower where there is ice. The change here is small, and not of the same order as when the sea ice is removed. (check the sea ice anyway, is there a difference between sea ice in control and sea ice in aero 10?

The longwave cloud emissivity is sensitiv to an increase in water amount as long as the LWP is less than $\approx 40\text{-}45 \text{ g/m}^2$. It is clear in Day 5 from the control run that the LWP was around $60\text{-}100 \text{ g/m}^2$ in the middle lower area of the figure@ (around these lat and lon?@). This is also seen in that there is no significant change in LW downward at the surface or upward at the TOA (see figures@). The area with lack of change in LW up or down is approximately the same area as where there is a negative change in LH and SH upward from the surface over the sea ice. Since there has been no change in LW there is no loss of warming from a decrease in LW reaching the surface, but the change can be explained by looking at the SW radiation(@figures). The downward SW at the surface has been significantly decreased as a consequence of the increase in aerosols. The SW radiation has been reflected by the smaller and more numerous droplets(@figures). This is known as the Twomey effect, and was described in Chapter 2. The albedo of sea ice is typically (@numbers) which means that a small fraction of the incident SW radiation is absorbed. Since the amount of incident SW radiation at the surface has been reduced by the cloud cover, the absorbed radiation is less than for a higher incident amount. The ice therefore has a lower temperature to give off SH with.

Look at temperature changes at the surface. Over ice and ocean.. The SSTs are the same for all the runs and there is no coupling with the ocean. The skin temperature for the domain shows a small decrease in the same area as where there is less sensible and latent heat release.

Also the dynamics over ice and the ocean are different, so this could have an effect. The cold air over the ice may be intensified, while the warmer air over the ocean would not change due to SST-changes, so the response may be smaller there...?

4.6 The control run figures!

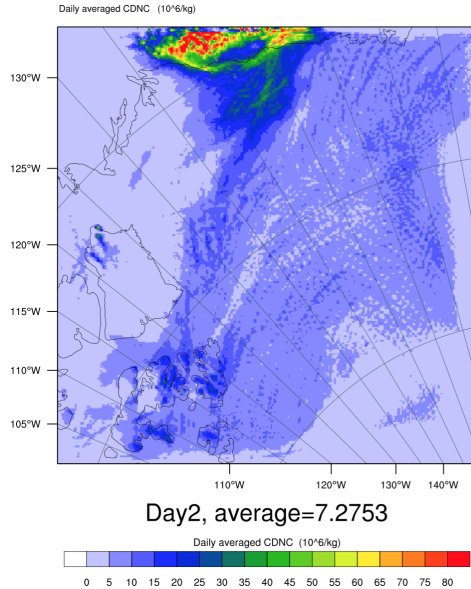


Figure 4.6: Cloud droplet number concentration, plottet over the area, averaged over the lower 11 layers on the 5th day.

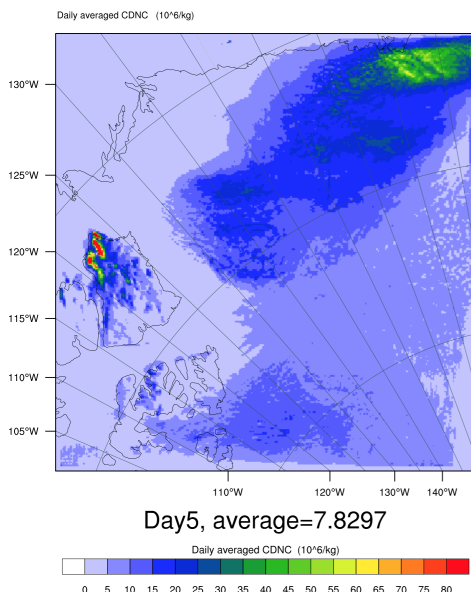


Figure 4.7: Cloud droplet number concentration, plottet over the area, averaged over the lower 11 layers on the 5th day.

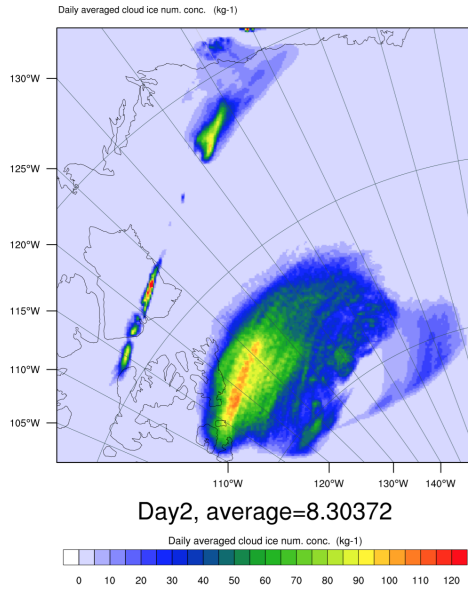


Figure 4.8: Cloud ice number concentration, plottet over the area, averaged over the lower 11 layers on the 5th day.

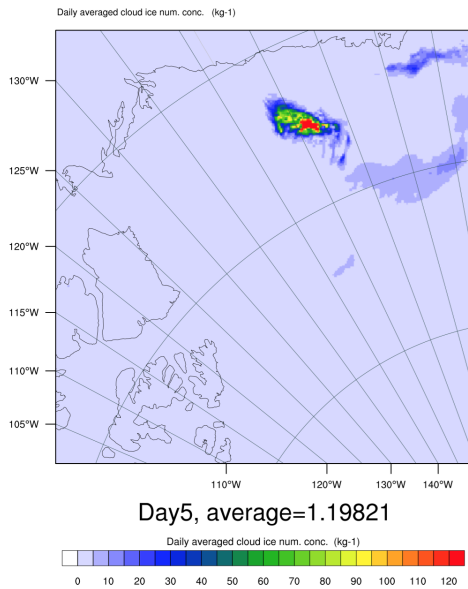


Figure 4.9: Cloud ice number concentration, plottet over the area, averaged over the lower 11 layers on the 5th day.

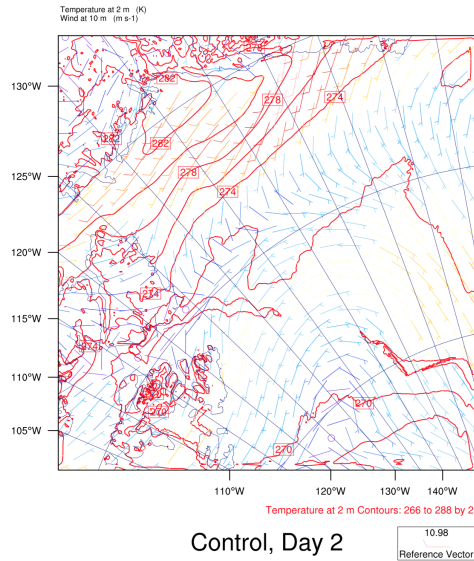


Figure 4.10: Map showing the mean wind at 10 m as wind barbs and mean temperature at 2 m as contours, for day 2 of the control run.

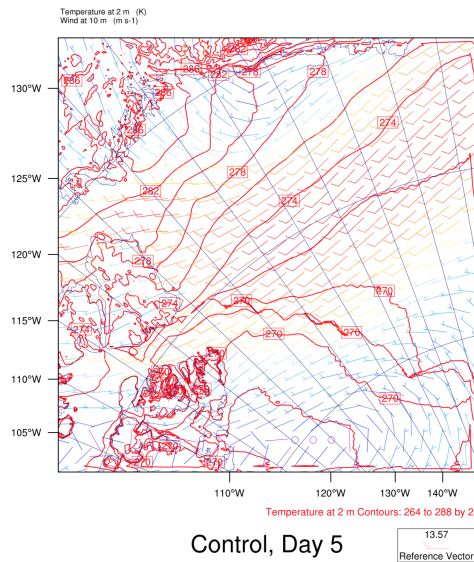


Figure 4.11: Map showing the mean wind at 10 m as wind barbs and mean temperature at 2 m as contours, for day 5 of the control run.

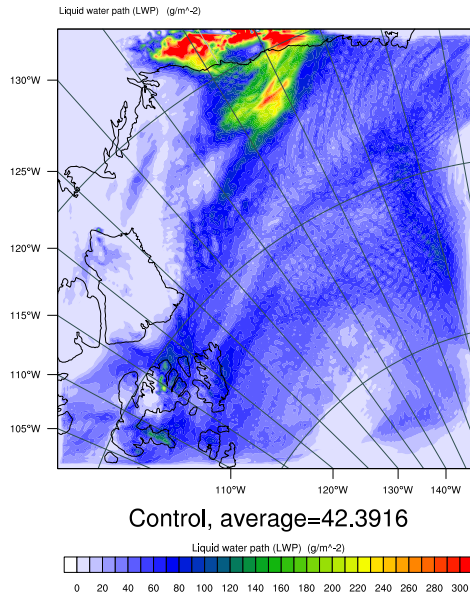


Figure 4.12: The liquid water path (LWP) average field for day 2 of the control run, with the average value for that field.

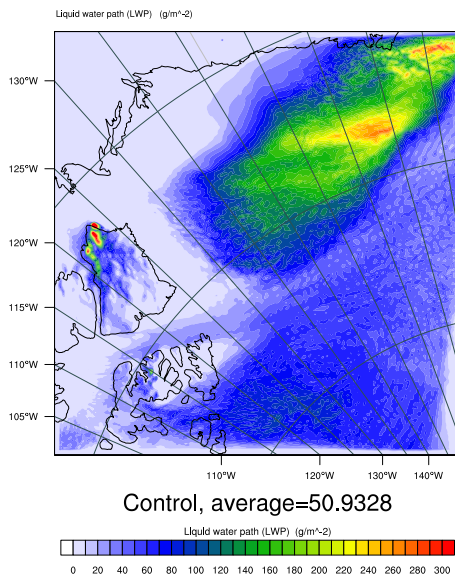


Figure 4.13: The liquid water path (LWP) average field for day 2 of the control run, with the average value for that field.

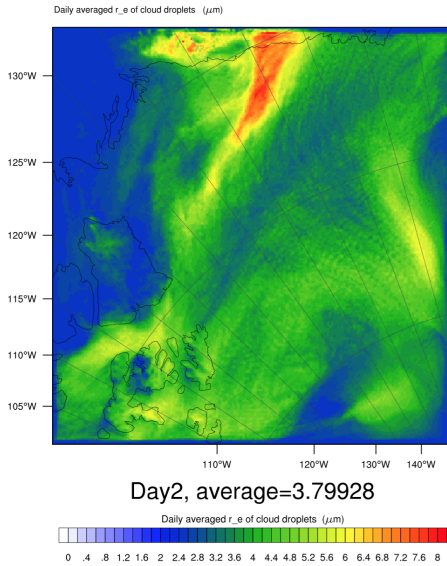


Figure 4.14: The effective radius of cloud droplets average field for day 2 over the lowermost 11 layers.

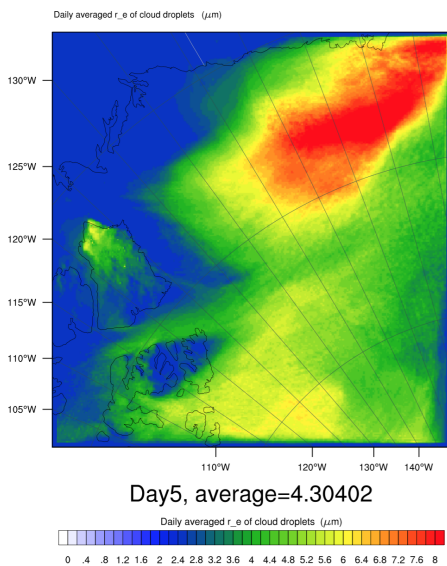


Figure 4.15: The effective radius of cloud droplets average field for day 2 over the lowermost 11 layers.

Chapter 5

Summary and Conclusions

In this thesis I have found that what happens in the model fits well with the theory. When the atmosphere has not yet adapted to the removal of sea ice or increase in aerosols, it is

Bibliography

- Aguado, Edward, & Burt, James E. 2010. *Understanding Weather and Climate*. 5th edn. Pearson Prentice Hall.
- Albrecht, Bruce A. 1989. Aerosols, Cloud Microphysics, and Fractional Cloudiness. *Science*, **245**(4923), 1227–1230.
- Beitler, Jane. 2012. Arctic sea ice extent settles at record seasonal minimum. *National Snow and Ice Data Centre U.S.A.*
- Boucher, O., Randall, David, Artaxo, P., Bretherton, C., Feingold, G., Forster, P., Kerminen, V.M., Kondo, Y., Liao, H., Lohmann, U., Rasch, P., Satheesh, S. K., Sherwood, S., Stevens, B., & Zhang, X. Y. 2013. Clouds and Aerosols. Pages 571–657 of: Stocker, T. F., Qin, D., Plattner, G.-K., Tignor, M., Allen, S.K., Boschung, J., Nauels, A., Xia, Y., Bex, V., & Midgley, P. M. (eds), *Climate Change 2013: The physical Science Basis. Contribution of Working Group I to the Fifth Assessment Report of the Intergovernmental Panel on Climate Change*. Cambridge University Press, Cambridge, United Kingdom and New York, NY, USA.
- Curry, J. a., Hobbs, P. V., King, M. D., Randall, D. a., Minnis, P., Isaac, G. a., Pinto, J. O., Uttal, T., Bucholtz, A., Cripe, D. G., Gerber, H., Fairall, C. W., Garrett, T. J., Hudson, J., Intrieri, J. M., Jakob, C., Jensen, T., Lawson, P., Marcotte, D., Nguyen, L., Pilewskie, P., Rangno, A., Rogers, D. C., Strawbridge, K. B., Valero, F. P. J., Williams, a. G., & Wylie, D. 2000. FIRE arctic clouds experiment. *Bulletin of the American Meteorological Society*, **81**(1), 5–29.
- Curry, Judith A., Schramm, Julie L., Rossow, William B., & Randall, David. 1996. Overview of Arctic Cloud and Radiation Characteristics. *Journal of Climate*, **9**(8), 1731–1764.
- Eastman, Ryan, & Warren, Stephen G. 2010a. Arctic cloud changes from surface and satellite observations. *Journal of Climate*, **23**(15), 4233–4242.

- Eastman, Ryan, & Warren, Stephen G. 2010b. Interannual variations of arctic cloud types in relation to sea ice. *Journal of Climate*, **23**(15), 4216–4232.
- Graversen, Rune G, Mauritsen, Thorsten, Tjernström, Michael, Källén, Erland, & Svensson, Gunilla. 2008. Vertical structure of recent Arctic warming. *Nature*, **451**(7174), 53–56.
- Hansen, J. E., & Travis, L. D. 1974. Light scattering in planetary atmospheres. *Space Science Reviews*, **16**(1957), 527–610.
- Iacono, Michael J. 2003. Evaluation of upper tropospheric water vapor in the NCAR Community Climate Model (CCM3) using modeled and observed HIRS radiances. *Journal of Geophysical Research*, **108**(D2).
- Iacono, Michael J., Mlawer, Eli J., Clough, Shepard a., & Morcrette, Jean-Jacques. 2000. Impact of an improved longwave radiation model, RRTM, on the energy budget and thermodynamic properties of the NCAR community climate model, CCM3. *Journal of Geophysical Research*, **105**(D11), 14873.
- Iacono, Michael J., Delamere, Jennifer S., Mlawer, Eli J., Shephard, Mark W., Clough, Shepard a., & Collins, William D. 2008. Radiative forcing by long-lived greenhouse gases: Calculations with the AER radiative transfer models. *Journal of Geophysical Research: Atmospheres*, **113**(13), 2–9.
- Intrieri, J M, Shupe, M D, Uttal, T, & Mccarty, B J. 2002a. An annual cycle of Arctic cloud characteristics observed by radar and lidar at SHEBA. *Journal of Geophysical Research*, **107**(C10).
- Intrieri, J. M., Fairall, C. W., Shupe, M. D., Persson, P. Ola G, Andreas, E. L., Guest, P. S., & Moritz, R. E. 2002b. An annual cycle of Arctic surface cloud forcing at SHEBA. *Journal of Geophysical Research*, **107**(C10), 1–14.
- Kay, Jennifer E., & Gettelman, Andrew. 2009. Cloud influence on and response to seasonal Arctic sea ice loss. *Journal of Geophysical Research D: Atmospheres*, **114**(18).
- Klein, S. A., & Hartmann, D. L. 1993. The seasonal cycle of low stratiform clouds. *Journal of Climate*, **6**, 1587–1606.

- Liou, K. N. 2002. *An Introduction to Atmospheric Radiation*. 2nd edn. Academic Press.
- Lohmann, U., & Feichter, J. 2005. Global indirect aerosol effects: a review. *Atmospheric Chemistry and Physics Discussions*, **4**(6), 7561–7614.
- McDonald, James E. 1958. *The Physics of Cloud Modification*.
- Mlawer, Eli J., Taubman, Steven J., Brown, Patrick D., Iacono, Michael J., & Clough, Sheppard a. 1997. Radiative transfer for inhomogeneous atmospheres: RRTM, a validated correlated-k model for the longwave. *Journal of Geophysical Research*, **102**(D14), 16663.
- Palm, Stephen P., Strey, Sara T., Spinhirne, James, & Markus, Thorsten. 2010. Influence of Arctic sea ice extent on polar cloud fraction and vertical structure and implications for regional climate. *Journal of Geophysical Research*, **115**(D21), D21209.
- Reisner, J, Rasmussen, R M, & Bruintjes, R T. 1998. Explicit forecasting of supercooled liquid water in winter storms using the MM5 mesoscale model. *Quarterly Journal of the Royal Meteorological Society*, **124**(548), 1071–1107.
- Rogers, R. R., & Yau, M. K. 1989. *A Short Course in Cloud Physics*. 3rd edn. Butterworth-Heinemann.
- Schweiger, Axel J., Lindsay, Ron W., Vavrus, Steve, & Francis, Jennifer A. 2008. Relationships between Arctic Sea Ice and Clouds during Autumn. *Journal of Climate*, **21**(18), 4799–4810.
- Shupe, Matthew D., & Intrieri, Janet M. 2004. Cloud radiative forcing of the Arctic surface: The influence of cloud properties, surface albedo, and solar zenith angle. *Journal of Climate*, **17**(3), 616–628.
- Skamarock, William C., & Klemp, Joseph B. 2008. A time-split nonhydrostatic atmospheric model for weather research and forecasting applications. *Journal of Computational Physics*, **227**(7), 3465–3485.
- Thompson, Gregory, & Eidhammer, Trude. 2014. A study of aerosol impacts on clouds and precipitation development in a large winter cyclone. *Journal of the Atmospheric Sciences*, 140507124141006.
- Thompson, Gregory, Rasmussen, Roy M., & Manning, Kevin. 2004. Explicit Forecasts of Winter Precipitation Using an Improved Bulk Microphysics

- Scheme. Part I: Description and Sensitivity Analysis. *Monthly Weather Review*, **132**, 519–542.
- Thompson, Gregory, Field, Paul R., Rasmussen, Roy M., & Hall, William D. 2008. Explicit Forecasts of Winter Precipitation Using an Improved Bulk Microphysics Scheme. Part II: Implementation of a New Snow Parameterization. *Monthly Weather Review*, **136**, 5095–5115.
- Twomey, S. 1974. Pollution and the Planetary Albedo. *Atmospheric Environment*, **8**, 1251–1256.
- Twomey, S. 1977. The Influence of Pollution on the Shortwave Albedo of Clouds. *Journal of the Atmospheric Sciences*, **34**, 1149–1152.
- Uttal, Taneil, Curry, Judith a., Mcphee, Miles G., Moritz, Donald K. Perovich Richard E., Maslanik, James a., Guest, Peter S., Stern, Harry L., Moore, James a., Turenne, Rene, Heiberg, Andreas, Serreze, Mark. C., Wylie, Donald P., Persson, Ola G., Paulson, Clayton a., Halle, Christopher, Morison, James H., Wheeler, Patricia a., Makshtas, Alexander, Welch, Harold, Shupe, Matthew D., Intrieri, Janet M., Stamnes, Knut, Lindsey, Ronald W., Pinkel, Robert, Pegau, W. Scott, Stanton, Timothy P., & Grenfeld, Thomas C. 2002. Surface heat budget of the Arctic Ocean. *Bulletin of the ...*, 255–276.
- Vavrus, Steve, Holland, Marika M., & Bailey, David A. 2010. Changes in Arctic clouds during intervals of rapid sea ice loss. *Climate Dynamics*, **36**, 1475–1489.
- Verlinde, J., Harrington, J. Y., McFarquhar, G. M., Yannuzzi, V. T., Avramov, a., Greenberg, S., Johnson, N., Zhang, G., Poellot, M. R., Mather, J. H., Turner, D. D., Eloranta, E. W., Zak, B. D., Prenni, a. J., Daniel, J. S., Kok, G. L., Tobin, D. C., Holz, R., Sassen, K., Spangenberg, D., Minnis, P., Tooman, T. P., Ivey, M. D., Richardson, S. J., Bahrmann, C. P., Shupe, M., DeMott, P. J., Heymsfield, a. J., & Schofield, R. 2007. The mixed-phase arctic cloud experiment. *Bulletin of the American Meteorological Society*, **88**(2), 205–221.
- Wang, Wei, Bruyère, Cindy, Duda, Michael, Dudhia, Jimy, Gill, Dave, Kavulich, Michael, Keene, Kelly, Lin, Hui-Chuan, Michalakes, John, Rizvi, Syed, Zhang, Xin, Berner, Judith, & Smith, Kate. 2015. *WRF ARW Version 3 Modeling System User's Guide*. Mesoscale & Microscale Meteorology Division, National Centre for Atmospheric Research.

- Wu, Dong L., & Lee, Jae N. 2012. Arctic low cloud changes as observed by MISR and CALIOP: Implication for the enhanced autumnal warming and sea ice loss. *Journal of Geophysical Research: Atmospheres*, **117**(D7).